Characterization of the Membranes in the Giant Nerve Fiber of the Squid

RAIMUNDO VILLEGAS and GLORIA M. VILLEGAS

From Laboratorios de Biofísica y de Ultraestructura, Instituto Venezolano de Investigaciones Científicas, (I.V.I.C.), Caracas, Venezuela

There are several methods by which the structure of a cell may be studied. The electron microscope makes it possible to visualize details of the ultrastructure, and to resolve these details with a resolution of 10 Å. Membranes may also be characterized in terms of the molecules which diffuse across them, leading to a resolution which may be an order of magnitude greater. It is the object of the present study to examine the giant nerve fiber of the squid by both of these methods to see if the combination will clarify the picture of the nerve membrane. The questions to be explored are: (1) are there any channels in the Schwann cell which have not been previously detected? (2) where is the barrier to the diffusion of water into the axoplasm? (3) are the barriers to diffusion and filtration the same? and (4) can the axolemma be characterized in terms of an equivalent pore radius? The final point of inquiry is whether the structure thus elucidated bears any relation to the ion transport mechanism which has already been so thoroughly explored (1).

I. *Ultrastructure of the Giant Nerve Fiber*

EXPERIMENTAL PROCEDURE

The giant nerve fibers from the first stellar nerve of the tropical squid *Doryteuthis plei* were used. After separation of the giant fiber from the rest of the bundle, both its ends were tied with thread and sectioned. Less than 10 minutes were spent in the whole isolation procedure. The nerve fiber was immediately immersed in one of the two following ice-cold fixative solutions prepared in buffered veronal-acetate artificial sea water (*a*) 2 per cent OsO_4 (2) or (*b*) 0.6 per cent $KMnO_4$ (3). Both solutions had a pH of 8.0–8.1. The composition of the artificial sea water according to Hodgkin and Katz (4) is shown in Table I. An osmolarity of 1010 mOsM/liter as determined by a freezing point osmometer (Fiske osmometer apparatus), has been taken as isotonic with the nerve fiber. Most of the fibers were fixed under tension with small glass weights attached to the thread at one end. Some, however, were fixed without tension in order to discard this factor as a possible cause of artifacts.

A 2 hours' fixation period seems to be best for OsO_4, and 16 to 18 hours for the

$KMnO_4$. After washing in two changes of distilled water for the OsO_4-fixed material and 25 per cent ethanol for the $KMnO_4$-fixed material, the fibers were dehydrated in successive changes of ethanol. They were imbedded in a prepolymerized mixture of *n*-butyl and methyl methacrylate. The polymerization was carried out at 60°C. (5). Fine sections were cut in a Moran ultramicrotome equipped with diamond knife (6). They were mounted on formvar or carbon films with holes in order to provide better contrast (7) and examined with a Siemens Elmiskop I electron microscope.

TABLE I

COMPOSITION OF ISOTONIC AND HYPOTONIC ARTIFICIAL SEA WATER

	Isotonic		Hypotonic	
	gm./liter	*mM/liter*	*gm./liter*	*mM/liter*
NaCl	25.82	441.7	20.66	353.4
KCl	0.74	9.9	0.74	9.9
$CaCl_2 \cdot 2H_2O$	1.61	11.0	1.61	11.0
$MgCl_2 \cdot 6H_2O$	10.80	53.1	10.80	53.1
$NaHCO_3$	0.21	2.5	0.21	2.5
Osmolarity* (mOsM./liter)		1010		805
C_{iso}		1.00		0.80
pH		8.1		8.0

* Measured by freezing point depression, using NaCl standards with osmolarity corrected for activity coefficients.

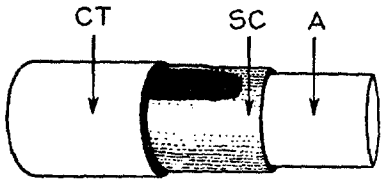

TEXT-FIGURE 1. Schematic drawing showing the relation between axon (*A*), Schwann cell (*SC*), and connective tissue (*CT*), in the nerve fiber of the squid.

Text-fig. 1 shows the relation between axon, Schwann cell, and connective tissue diagramatically; Fig. 1 shows the electron microscope picture.

THE AXON STRUCTURE

Examination of electron micrographs[1] reveals that the axoplasm contains filaments 50 to 70 Å long, running in all directions with a predominantly longitudinal arrangement; they usually form bundles consisting of 5 or more filaments, making the axoplasm appear very dense (Fig. 1). The mitochondria are, in general, round formations of widely varying sizes with a number of tubular cristae in both longitudinal and transversal directions; they are mostly located in the periphery.

The axon is bound by a membrane, the axolemma, which consists of a pair

[1] Electron micrograph measurements have been increased in 15 per cent to correct for the shrinkage produced by the metachrilate embedding. Such corrected values are used in the present paper.

of dense lines, each line being ~27 Å thick, separated by a less dense space of ~25 Å, forming a unit of ~79 Å, as shown in Figs. 6 and 7. In the present paper special attention is given to the significance of this formation as the bounding membrane of the axon.

THE SCHWANN CELL STRUCTURE

The Schwann cell is separated from the axolemma by a space of ~83 Å (Figs. 6 and 7). The Schwann cell thickness varies from 0.1 to 0.2 μ near the ends to 0.8 to 0.9 μ in the region of the nucleus. The nucleus appears to be enlarged, having a rectangular shape which is uniformly dense in the periphery. Intensely osmiophilic corpuscles, bounded by a membrane, which seem to correspond to the Erholz bodies, have been observed in the vicinity of the nucleus. The perinuclear region of the cytoplasm also contains mitochondria, the Golgi complex, and many endoplasmic reticulum vesicles of various diameters.

The most characteristic aspect of the Schwann cell cytoplasm is the system of membranes described by Geren and Schmitt (8). In the material fixed with OsO_4 and observed at low resolution these membranes appear as 3 to 6 double-edged osmiophilic layers running parallel to the axon (Figs. 2 and 3). Frankenhaeuser and Hodgkin (9) have suggested that the less dense zones between those osmiophilic double lines were continuous aqueous channels through which contact is maintained between the axolemma and the extracellular medium. From the high resolution study in thin transversal and longitudinal sections of these double-edged layers in $KMnO_4$ and in OsO_4-fixed material, we (10) have shown that each edge can be described as a pair of dense lines ~27 Å each, separated by an intermediate less dense zone of ~25 Å. The two channel walls are separated from one another by a space, or channel lumen, of ~60 Å (Figs. 6 and 7). The structure of each channel wall is thus similar to that observed for the axolemma and the Schwann cell membrane (Figs. 6 and 7). These channels appear to be invaginations of the Schwann cell membrane as shown in Figs. 4, 5, 6, and 7. As previously stated (10, 11) some of these channels form a continuous pathway from one side of the Schwann cell to the other (Figs. 4, 5, and 6). In all probability there exist two or more kinds of channels (Text-fig. 2), some directly connecting the extracellular space with the space between the axolemma and the Schwann cell, while others terminate in a blind alley. The tortuous aspect of these channels makes it difficult to view them in thin sections.

From the study of both transversal and longitudinal sections a three-dimensional view of the Schwann cell channels has been obtained. They seem to be large slits as shown in Text-fig. 3. The length of the path connecting one side of the Schwann cell to the other has been determined for two channels in the same transversal section, 4.5 μ for one and 4.1 μ for the other. Since the thickness of the Schwann cell in this region is about 0.5 μ, the channel length is

some eight times greater than the cell thickness. The channel lumen has a cross-section whose width, as previously stated, is ~60 Å, and whose length is 5.3 μ, an average of four measurements.

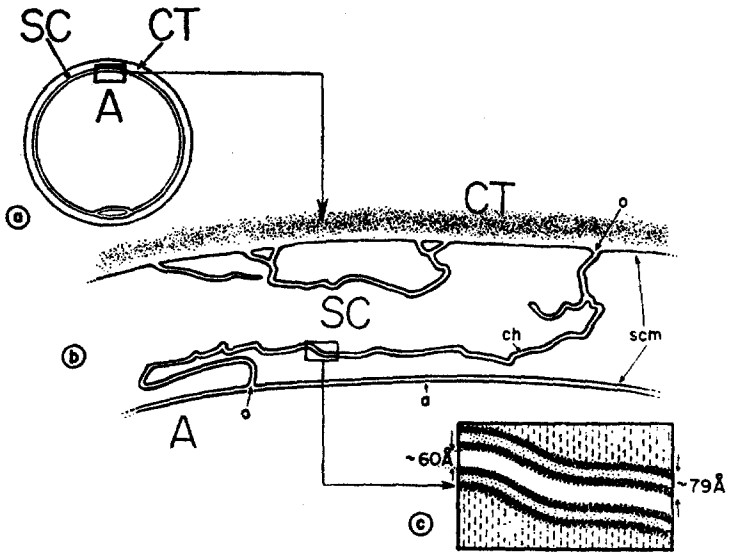

TEXT-FIGURE 2. Schematic drawing showing axon-Schwann cell relationship in the squid giant fiber. (*a*) Relation between axon (*A*), Schwann cell (*SC*), and connective tissue (*CT*), as shown in cross-section. (*b*) Enlarged portion of fiber in the boundary region between axon (*A*), Schwann cell (*SC*), and connective tissue (*CT*). Special attention is called to the intracytoplasmatic channels (*ch*) in the Schwann cell. Some of the channels (*ch*) form a continuous pathway with two openings (*o*), one in the space between axon surface (axolemma = *a*) and Schwann cell, the other in the extracellular space (connective tissue). Another channel appears ending in a blind alley. The continuity of the Schwann cell membrane (*scm*) with the channel walls can also be seen. (*c*) Highly enlarged portion of a channel showing the fine structure of walls as observed in OsO_4- and $KMnO_4$-fixed material, with high resolution electron microscopy. Each wall appears as a membrane unit formed by two dense lines separated by a less dense one. Walls are separated from one another by a 60 Å channel lumen. The dimensions are from electron micrograph measurements with a 15 per cent increase, taking into consideration the metachrylate embedding.

The individuality of the Schwann cell has been previously demonstrated (10). Covering the Schwann cell is a homogeneous layer of low density, 0.1 to 0.2 μ thick, which has been called basement membrane (Fig. 1) by Geren and Schmitt (8). Outside this structure, there are connective tissue cells and collagen bundles which become rarer as they withdraw from the nerve fiber. This homogeneous low density structure should not properly be called a membrane, since it does not form a continuous structured barrier, as is the one for the Schwann cell membrane.

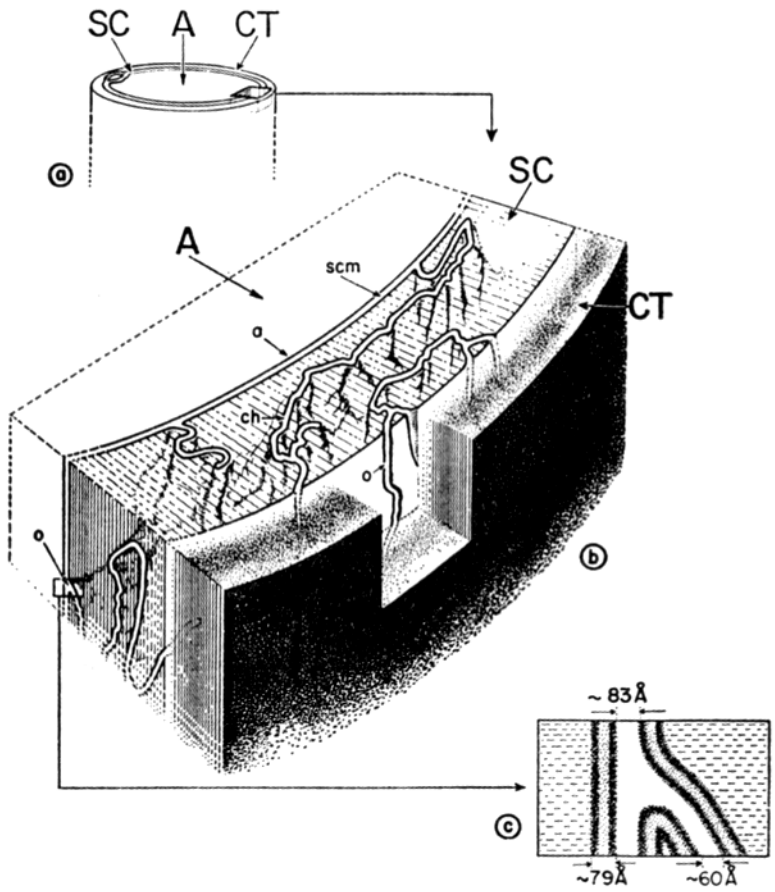

TEXT-FIGURE 3. Three-dimensional diagram of the giant nerve fiber of the squid. (*a*) A segment of the nerve fiber showing the axon (*A*) covered by the Schwann cell (*SC*). The latter is covered by the connective tissue (*CT*). (*b*) Enlarged portion of the fiber in which channels (*ch*) are shown as slits crossing the Schwann cell from outer surface to axonal surface. Special attention is called to the openings (*o*) of the channels (*ch*). It may be seen that some of the channels which in ultrathin sections (diagram of Text-fig. 2) appear ending in a blind alley, are found to be continuous at different levels, as has been observed in serial electron micrographs. (*c*) Highly enlarged view of one of the channel openings (*o*) in which the continuity of the channel walls with the Schwann cell membrane (*scm*) is demonstrated. The fine structure of the axolemma (*a*) is shown. No difference can be appreciated between this structure (*a*), the Schwann cell membrane (*scm*), and the channel wall structure (*ch*).

BEHAVIOR OF SCHWANN CELL CHANNELS IN HYPOTONIC MEDIUM

Preliminary results were obtained on two different fibers which were left for 10 minutes in hypotonic sea water (805 mOsM/liter) and then fixed in buffered 0.6 per cent $KMnO_4$ solution of the same osmolarity. Under hypotonic

conditions some alterations in the channels have been observed resulting from swelling of the Schwann cell. In some places the channel is occluded but a continuous path still connects the two sides of the Schwann cell. The structural pattern (Figs. 8 and 9) shows three dense lines in some regions instead of four. The center line, caused by fusion of the channel walls, includes the inside dense line of each wall. In serial sections the channel path is clearly continuous, so that communication between the extracellular space and the axolemma is not interrupted. Since the channel width responds to osmotically induced forces, it would seem likely that the channel lumen is filled with water and ions which can be squeezed out when the Schwann cell swells, rather than with material of very high viscosity which would largely retain its initial volume in the face of the osmotic forces.

II. *Diffusion of Water into the Giant Nerve Fiber*

EXPERIMENTAL PROCEDURE

Once the fiber is dissected, the ends are tied with waxed thread. The thread which ties one of the ends is cut close to the loop. The other is threaded through a capillary tube which is then sealed with wax at both ends so that, in effect, the tube serves as a means of handling the preparation. The axon diameter and the fiber length are measured as described in section III.

The fiber is then passed to a holder containing 10 ml. of artificial isotonic sea water, made up with tritium. For the preparation of radioactive sea water, tritiated water having an activity of 2 mc. per ml. is used instead of ordinary water. The fiber is left in this solution for 15 minutes, by which time tracer equilibrium has been reached. The fiber is then blotted and immediately soaked in a series of thirteen baths, each containing 2 ml. of non-radioactive artificial sea water. The length of time in seconds in each bath, measured by a chronometer, is successively: 5, 10, 15, 30 (four baths), 60, 120 (four baths), and 600 seconds. It is estimated that the fiber remains in air less than 1 second as it is passed from one bath to the other. The temperature varied between 22° and 24°C.

DETERMINATION OF TRITIUM

The concentration of tritium in the artificial radioactive sea water and in each of the baths is determined by a liquid scintillation counter (Tri-Carb spectrometer, model 314). The bath fluid in each flask was added to 10 ml. of scintillation solution of the following composition:

2,5-Diphenyloxazole	3.00 gm.
1,4-Di-2-(5-phenyloxazolil)-benzene	0.10 gm.
Naphthalene	50.00 gm.
Made up to 1000 ml. with dioxane	

Counting was performed at 4°C., with the pulse height discriminators set to receive pulses of 10 to 100 volts, and photomultiplier voltages of 1200 volts.

The standard deviation in net counting was less than 1 per cent. The flasks were discarded after each experiment, to prevent effects caused by residual radioactivity.

CALCULATION OF TRITIATED WATER CONCENTRATION OF EACH BATH

Having determined the specific activity of the tritiated sea water into which the fiber was originally placed (denoted as standard H^3 sea water), the volume of tritiated water in each bath may be determined as follows:

$$\frac{\text{C.P.M. of the bath}}{\text{C.P.M./cm.}^3 \text{ of standard } H^3 \text{ sea water}} = \text{cm.}^3 \text{ of tritiated water in the bath}$$

in which C.P.M. means counts per minute.

MATHEMATICAL TREATMENT OF THE DATA

The tritiated water collected in each bath is the volume that has left the fiber during the time of washing. By plotting the cumulative volume of radioactive water as a function of time, a curve such as that of Text-fig. 4 is obtained.

The equations to be presented describe water diffusion across the nerve fiber membrane under the following assumptions:

(*a*) The system is properly described as two compartments in series, which open at one end only into an infinitely large volume of non-radioactive artificial isotonic sea water (Text-fig. 5), the return of radioactivity to the nerve fiber being negligible. The compartments are thus: (1) the axon, (2) the extracellular fluid, and (3) the bathing sea water;
(*b*) The nerve fiber compartments behave as well mixed compartments;
(*c*) The volume of the compartments within the nerve fiber remain constant during the experiment;
(*d*) Tritiated water ($H^1H^3O^{16}$), after suitable correction, acts as an ideal tracer for ordinary water ($H^1_2O^{16}$); and
(*e*) Radiation from the tritium does not alter the activity of the nerve.

The assumption that the nerve fiber is essentially composed of two compartments in series open at one end only is based on the biological structure of the preparation itself. The inner compartment must be represented by the axon, the outer by the extracellular space, through which necessarily any element originating in the axon must pass to reach the bath. This would be in essence a two-compartment system open at one end (11, 12), instead of a parallel system of two compartments, both of them opening in the bath water, as implied in Nevis' work (13).

The adequacy of mixing in the axon interior and extracellular space can not be measured experimentally, but may be estimated by calculation. For

good mixing, the rate of diffusion in each compartment should be large compared with the rate of exchange across the relevant compartment boundary. Diffusion out of a cylinder is characterized by a multi-exponential curve, as is the rate of exchange across the boundaries. Consequently a graphical comparison of the two processes provides a convenient method of comparison.

The equation for diffusion out of a cylinder in which the length is much greater than the diameter is given by Jacobs (14) as:

$$\frac{p^*}{p^*_0} = 4\left[\frac{e^{-(Dv_1^2 t/r_0^2)}}{v_1^2} + \frac{e^{-(Dv_2^2 t/r_0^2)}}{v_2^2} + \cdots\right] \qquad (1)$$

in which p^* is the average specific activity in the axon interior, p^*_0 is the initial

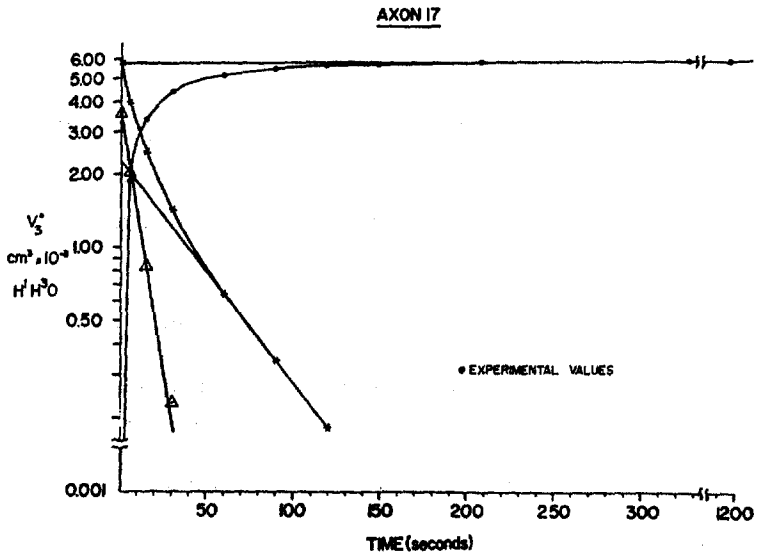

TEXT-FIGURE 4. Tritiated water efflux from a giant nerve fiber of the squid. The cumulative volume of radioactive water recovered in a series of large non-radioactive isotonic sea water baths are plotted as a function of time. The experimental curve is found to consist of a fast and a slow phase. In the text, C_1 is the intersection of the fast phase on the ordinate axis and C_2 that of the slow phase; r_1 and r_2 are the slopes of the fast and slow phases respectively.

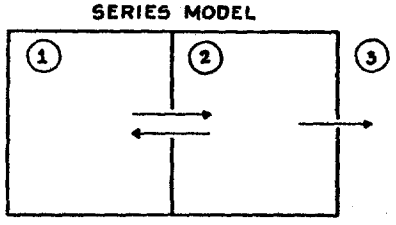

TEXT-FIGURE 5. Arrangement of compartments for theoretical analysis of data; (1) axon; (2) extracellular fluid; and (3) bathing sea water.

specific activity in the axon, D is the diffusion coefficient of tritiated water in the axon interior, r_0 is the axon diameter, v_1 and v_2 are the zeros of the Bessel's function of zero order with the values of 2.405 and 5.520 respectively. D within the axon is unknown, but may be assumed to approximate the diffusion coefficient of $H^1H^3O^{16}$ in ordinary water at 23°C. which is equal to 2.28×10^{-5} cm.^{2}/sec. as obtained by graphical interpolation from the data of Wang, Robinson, and Edelman (15). In an axon 3.0×10^{-2} cm. in diameter, p^* would fall to 50 per cent of its initial value in 1 second (the terms of higher order in equation 1 may be neglected). During this period of time the specific activity of the axon interior falls by only 3 per cent as calculated from typical experimental data by equation 6 given below. Thus it would appear that diffusion is not the rate-limiting step governing the movement of tritiated water out of the axon.

It is also possible to approximate diffusion in the extracellular space, if it is considered as a plane liquid sheet covering the axon. Roughton's (16) treatment of the diffusion of oxygen in the red cell interior as adapted by Paganelli and Solomon (17) for tritiated water diffusion in the same cell has been used. In both treatments the red cell is considered as a plane liquid sheet, as has been done for the extracellular space in the present case. Since exchange between the extracellular space and the bathing medium is much faster than that between extracellular space and axon interior, the model should be altered to consider exchange across a single boundary of the plane only. This may be accomplished formally by using the following equation with a thickness set at double the actual thickness of the extracellular space (14):

$$\frac{p^*}{p^*_0} = 1 - \frac{8}{\pi^2} e^{-(D\pi^2/4b^2)t} \qquad (2)$$

in which p^* is the average specific activity of tritiated water in the extracellular space. For b, the half-thickness of the sheet, we have taken 0.5×10^{-2} cm., twice the typical half-thickness. Under these conditions p^* would fall to half its initial value in 0.3 second. During this period of time the specific activity of the extracellular space falls by only 1 per cent, as calculated from typical experimental data using equation 7 below. These considerations would lead to the conclusion that diffusion does not limit the exchange of tritiated water between the extracellular space and the bathing medium.

The assumption that the axon and the extracellular space remain of the same size throughout the experiment has been tested experimentally. No changes have been observed in the axon diameter and the connective tissue thickness, during one-hour exposure to isotonic sea water. The axon diameter was determined as routine with an accuracy of 2 μ; during the first 20 minutes the bathing sea water was changed every minute to imitate as closely as possible the actual experimental conditions. Since osmotic water shifts can

have some influence on the water exchange rate (18), care was taken to keep the osmolarity of the isotonic artificial sea water as constant as possible.

The assumption that tritiated water acts as an ideal tracer for ordinary water is customarily replaced by the assumption that $H^1_2O^{18}$ is characterized by the same diffusion coefficient as $H^1_2O^{16}$; the relative difference in mass between O^{16} and O^{18} is much less than that between H^1 and H^3. Since the diffu-

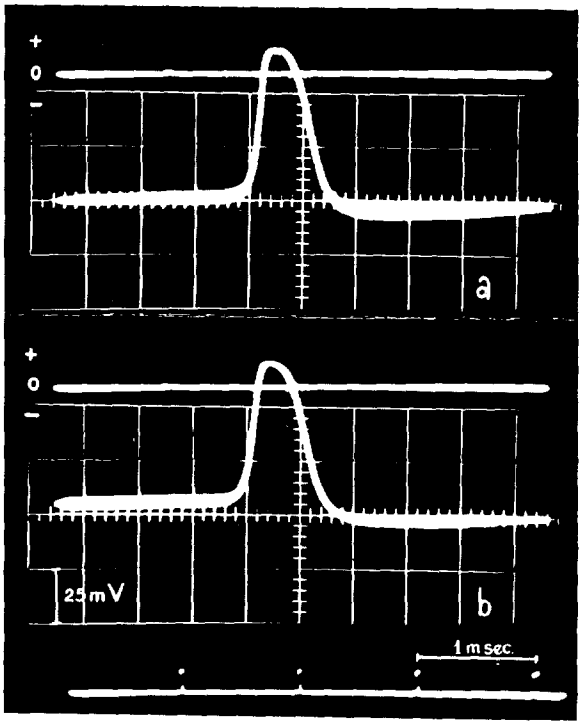

TEXT-FIGURE 6. (*a*) Resting and action potentials recorded between the inside and outside of an axon. After isolation the axon was immersed for a period of 2 hours in isotonic artificial sea water, prior to recording. (*b*) Resting and action potentials recorded from the same axon after immersion for 45 minutes in 15 ml. of tritiated sea water (specific activity, 2 mc. per ml.).

sion coefficient for $H^1_2O^{18}$ (obtained by graphical interpolation as previously discussed) is 14 per cent higher than that of $H^1H^3O^{16}$, the diffusion permeability coefficient obtained experimentally with tritiated water has also been increased by 14 per cent.

The importance of radiation effects may be assured experimentally. The resting and action potentials of a single axon immersed in 15 ml. tritiated water of the usual specific activity (2 mc./ml.) for 45 minutes are shown in Text-fig. 6, together with the values before tritium treatment. Since no variation in the electrical properties was observed under these conditions of exces-

sive exposure, it appears that radiation does not affect the physiological behavior of the tissue under normal experimental conditions.

On the basis of these considerations the following equations may be used to describe the rate of exchange of tritiated water volume with respect to time in compartments 1, 2, and 3:

$$\frac{dV^*_1}{dt} = -k_{12}V^*_1 + k_{21}V^*_2 \tag{3}$$

$$\frac{dV^*_2}{dt} = -(k_{21} + k_{23})V^*_2 + k_{12}V^*_1 \tag{4}$$

$$\frac{dV^*_3}{dt} = k_{23}V^*_2 \tag{5}$$

In these equations V^*_1, V^*_2, and V^*_3 are the volume of radioactive water in compartments 1, 2, and 3; k_{12}, k_{21}, and k_{23} are the rate constants which represent the fraction of compartmental water exchanging in unit time (the first and second subscripts refer to the compartment of origin and destination respectively), and t is the time.

The general solution of the system of equations 3, 4, and 5 has the form:

$$V^*_1 = A_1e^{-r_1t} + A_2e^{-r_2t} \tag{6}$$

$$V^*_2 = B_1e^{-r_1t} + B_2e^{-r_2t} \tag{7}$$

$$V^*_3 = -C_1e^{-r_1t} - C_2e^{-r_2t} + C_3 \tag{8}$$

Equation 8 describes the experimental curve (Text-fig. 4).

The relationship between the r's and the k's is shown by an auxiliary equation which occurs as a step in the solution of the system of equations 3, 4, and 5:

$$r^2 - (k_{12} + k_{21} + k_{23})r + k_{12}k_{23} = 0 \tag{9}$$

When equation 5 and the first derivative of equation 8 are evaluated at $t = 0$, k_{23} can be defined in terms of the C's, r's, and V_2, the volume of compartment 2 ($V_2 = V^*_{20} = V^*_2$ at $t = 0$):

$$k_{23} = \frac{r_1C_1 + r_2C_2}{V_2} \tag{10}$$

Using equations 9 and 10, the rate constants for exchange between compartments 1 and 2 in terms of the r's and k_{23} are obtained:

$$k_{12} = \frac{r_1r_2}{k_{23}} \tag{11}$$

$$k_{21} = r_1 + r_2 - (k_{12} + k_{23}) \tag{12}$$

Huxley's (19) treatment of the exchange of a labelled ion between certain tissues (muscle and nerve) and their surrounding medium has been adapted for the calculation of the volume of the compartments. It is possible to show that the volume of 1 is obtained according to the equation:

$$V_1 = V^*_{10} = \frac{C_1 C_2 (r_1 - r_2)^2}{C_1 r_1^2 + C_2 r_2^2} \tag{13}$$

Since V^*_3 at $t = \infty$ is equal to $V^*_{10} + V^*_{20}$ (the second subscript refers to time), the volume of compartment 2 is:

$$V_2 = V^*_{20} = V^*_{3\infty} - V^*_{10} \tag{14}$$

The tritiated water fluxes can be evaluated from the V's and the k's. The permeability coefficient for diffusion may be defined as the amount of water crossing the interphase per unit area:

$$P^*_d = \frac{k_{12} V_1}{A_m} = \frac{k_{21} V_2}{A_m} \tag{15}$$

in which A_m is the area of the membrane, and P^*_d is the permeability coefficient for tritiated water between compartments 1 and 2 in any direction ($P^*_{d12} = P^*_{d21}$).

The permeability coefficient for ordinary water between these compartments, P_d, may be obtained by increasing P^*_d by 14 per cent as previously discussed.

THE DIFFUSION PERMEABILITY COEFFICIENT

The values obtained for the rate constants and the compartmental volumes of 9 single nerve fiber preparations, in which the rate of exchange of tritiated water was followed under isosmotic conditions at a temperature of 22–24°C., are summarized in Table II.

The diffusion permeability coefficient (P_d) for ordinary water, between compartments 1 and 2, is calculated to be $1.42 \pm 0.39 \times 10^{-4}$ cm./sec. (Table III), the units being a measure of the volume of water, in cm.^{3}, that will cross 1 cm.^{2} of area in 1 second. This value may be compared with the results obtained by Nevis (13) for the giant axon of *Loligo pealii*. The model system Nevis used is different from the present one[2]; however, when his data

[2] In his text, Nevis (13) describes his model as a three-compartment system, comprising "one slow process between the axonal water and the connective tissue, and one faster process of exchange between the connective tissue and the surrounding isotonic solution." However, the equations which he uses to describe the system are those of a parallel open two-compartment system with no communication between the two compartments, axon water and connective tissue. In other words, his equations describe a system in which the only route of communication between axonal water and bathing medium is one which makes no contact with the extracellular fluid in the connective tissue.

(reference 13, Table V, nerve VIa) are calculated by our method, a value of 1.30×10^{-4} cm./sec. is obtained for *Loligo pealii*; this correspondence suggests that species differences are relatively unimportant with respect to the diffusion of water into the axon.

P_d is a measure of the fractional area for diffusion per unit path, according to: $P_d = -D_{H_2O}A/\Delta x$, in which D_{H_2O} is the diffusion coefficient of water, A the fraction of the total membrane area available for diffusion, and Δx the

TABLE II

THE VOLUME OF THE COMPARTMENTS AND THE RATE CONSTANTS FOR TRITIATED WATER EXCHANGE IN SINGLE NERVE FIBERS OF THE SQUID

(Temperature 22-24°C.)

Exp. No.	Axon area	Rate constants			Volume of the compartments	
		k_{12}	k_{21}	k_{22}	V_1	V_2
	$cm.^2$		$sec.^{-1} \times 10^{-2}$		$cm.^3 \times 10^{-6}$	
4	0.17	2.49	1.34	9.63	0.86	1.58
8	0.22	1.72	0.64	10.59	1.27	3.48
9	0.23	1.78	0.48	5.61	1.38	4.97
10	0.29	2.13	0.85	8.12	1.50	3.78
13	0.34	3.58	3.24	30.04	1.96	2.14
14	0.22	2.35	0.36	6.71	0.87	5.77
15	0.17	2.44	1.76	9.59	1.04	1.46
16	0.35	2.11	1.10	7.11	2.00	3.70
17	0.28	2.31	0.69	8.96	1.36	4.48

TABLE III

MEASUREMENTS OF P_d, THE PERMEABILITY COEFFICIENT FOR WATER DIFFUSION OUT OF SINGLE NERVE FIBERS OF THE SQUID

(Temperature 22-24°C.)

Exp. No.	Axon radius	P_d	P_d (in units of osmotic flow)
	$cm. \times 10^{-2}$	$(cm./sec.) \times 10^{-4}$	$\frac{ml.}{cm.^2, sec., cm.\ H_2O\ pressure} \times 10^{-10}$
4	1.47	1.44	1.04
8	1.50	1.14	0.83
9	1.78	1.20	0.87
10	1.50	1.26	0.91
13	1.59	2.34	1.70
14	1.45	1.07	0.78
15	1.71	1.71	1.24
16	1.60	1.35	0.98
17	1.45	1.27	0.92
Average ± Std. Dev.		1.42 ± 0.39	1.03 ± 0.29

length of the diffusion path. The diffusion coefficient of $H^1{}_2O^{18}$ at 23°C., as obtained by graphical interpolation from the data of Wang *et al.* (15) is 2.65×10^{-5} cm.²/sec. leading to a value of 5.3 cm. for $A/\Delta x$.

On theoretical grounds Frankenhaeuser and Hodgkin (9) postulated the existence of aqueous pathways between the excitable membrane and the external solution through which ions should move. For these channels, an $A/\Delta x$ of 4 cm. has been calculated by Frankenhaeuser and Hodgkin from the diffusion coefficient of potassium ions. Our figure of 5.3 calculated on the basis of water diffusion appears to agree closely with their value. The channel already shown in high resolution electron micrographs would seem, therefore, to be the operative extracellular barrier both for water and potassium diffusion. The total length of two of those channels was measured in electron micrographs giving values of 4.5 and 4.1 μ. If the average of these values may be taken as representative, we may estimate that only 0.23 per cent of the Schwann cell surface is required to permit the observed diffusion of water and potassium.

TABLE IV

VOLUME OF THE AXON OCCUPIED BY COMPARTMENT 1

Exp. No.	Axon volume	Volume ratio comp. 1/Axon
	$cm.^3 \times 10^{-4}$	
4	1.23	0.70
8	1.61	0.79
9	2.04	0.68
10	2.17	0.69
13	2.69	0.73
14	1.56	0.56
15	1.37	0.76
16	2.78	0.72
17	2.03	0.67
Average ± Std. Dev.		0.70 ± 0.07

WATER CONTENT OF THE AXON

The volume of compartment 1 expressed as a fraction of the axonal volume was found to be 0.70 ± 0.07, as shown in Table IV. The fraction of the axon volume which appears to be occupied by water is lower than the water contents determined by Koechlin (20) for the axoplasms extruded from a pool of giant axons of *Loligo pealii* (865 mg. per gm. of axoplasm). This discrepancy called for a determination of the content of water of the axoplasm of *Doryteuthis plei* by a different method. The axoplasms of single fibers were extruded

and collected on tared aluminum pans of about 1 mg. weight. They were immediately weighed in a quartz helix balance (Microchemical Specialties Co.) to a precision of ± 1 μg. Each sample was then dried to a constant weight by heating with infrared radiation. The temperature was never allowed to rise over 70°C. in the neighborhood of the sample, in order to avoid its decomposition.

The results obtained for the water contents of the axoplasms of 5 single axons which were calculated to be 773 ± 11 μg. per mg. of axoplasm, are presented in Table V. This value might be considered in fair agreement with that determined for compartment 1 by means of the diffusion kinetics experiments.

TABLE V

WATER CONTENT OF THE AXOPLASM OF SINGLE AXONS OF THE SQUID

Exp. No.	Axoplasm		
	Wet weight	Dry weight	Water content
	μg.	μg.	μg. per mg.
18	1038	231	777
19	380	82	784
20	401	92	770
21	1084	242	777
22	421	103	755
Average ± Std. Dev.			773 ± 11

III. *Entrance of Water under an Osmotic Pressure Gradient*

EXPERIMENTAL PROCEDURE

The isolated single nerve fibers are placed along specially made lucite holders containing isotonic sea water. They are kept slightly under tension by means of threads tied at both ends. The length is measured with 0.1 mm. precision with a vernier micrometer; each fiber is measured at least three times and the results always agree closely. The nerve fiber diameter is measured with a microscope equipped with an ocular micrometer, the divisions of which are standardized by a Zeiss stage micrometer. Each division of the ocular micrometer corresponds to 5.0×10^{-4} cm. and the image is sufficiently sharp to permit measurements with a precision of a third of a scale division. The large nerve fiber diameter did not allow further magnifications. The objective is immersed in the sea water, care being taken to avoid nerve fiber compression.

The experiments consist of measuring the changes from the original diameter of the axon in isotonic solution at varying intervals after the medium has been removed from the lucite chamber and replaced by a hypotonic solution. The composition of the solutions differ only in NaCl concentration, as shown in Table I. The length of

time the fiber is immersed in the hypotonic bath is measured by a chronometer, and observations are recorded at approximately 30, 80, 110, 155, 210, 280, 350, 420, and 600 seconds from the time the hypotonic medium made contact with the tissue; the timing error is approximately ± 1 second. Replacement in the isotonic environment was followed by return of the fiber to its initial diameter.

In some experiments (32 to 35) the nerve fibers were placed in solutions of different hypotonicity and only the initial (isotonic) and the final diameters were measured after equilibrium had been reached in the hypotonic solutions.

Results were accepted as valid when (*a*) the initial diameter was obtained after return to isotonic medium; (*b*) apparent microscopic alteration of the structure was not appreciable; and (*c*) conduction was preserved in the hypotonic environment.

MATHEMATICAL TREATMENT

The kinetics of water entrance under an osmotic pressure gradient in the absence of penetrating solutes, may be described by Jacobs' equation (reference 21, equation 2):

$$\frac{dV_w}{dt} = P_w A \left[\frac{C_0 V_{w0}}{V_w} - C_m \right] \tag{16}$$

in which V_w is the volume of axon water, expressed in milliliters; C and C_m are the concentration of solutes within the axon and the medium respectively, expressed in osmols per milliliter, the subscript 0 referring to initial conditions. A is the total nerve area in cm.^{2}, and t is the time. The filtration permeability coefficient, P_w, is a measure of the volume of water in cm.^{3} which flows across 1 cm.^{2} of surface in 1 second when a concentration gradient of 1 osM. per cm.^{3} is maintained. The term in square brackets represents the driving force where $(C_0 V_{w0}/V_w)$ defines the concentration of solutes within the axon since the product of the concentration and the volume of water within the cell is a constant:

$$C_0 V_{w0} = C V_w \tag{17}$$

Since the axon recovers its initial diameter when returned to isotonic sea water, the leakage of potassium or other solutes from the axon does not appear to be significant during the course of the experiment.

The experimental determination of osmotically induced water flow is obtained in terms of changes in axon volume. The cell volume is related to the water content of the cell by the following equation:

$$V_w = V_c - V_{c0}(1 - W_{eff}) \tag{18}$$

which is similar to that given by Sidel and Solomon (reference 22, equation 12). V_c is the axon volume, V_{c0} is V_c at $t = 0$, and W_{eff} is the axonal water which apparently participates in osmotic phenomena, expressed as a fraction of the cell volume.

As the nerve swells, changes in length can be avoided, or at least minimized, by applying tension to both ends of the fiber. Due to the irregularities of the axon surface in isotonic sea water the cell may swell with no changes in its area. The area of the nerve is issumed to remain constant for each experiment.

Introducing equation 18 into equation 16, the water entrance into the axon under an osmotic pressure gradient is described by the following equation:

$$\frac{dV_c}{dt} = P_w A \left[\frac{C_0 V_{c0} W_{eff}}{V_c - V_{c0}(1 - W_{eff})} - C_m \right] \tag{19}$$

Equation 19 may be integrated to give:

$$t = \frac{1}{P_w A C_m^2} \left[C_0 V_{c0} W_{eff} \ln \frac{V_{c0} W_{eff}(C_0 - C_m)}{C_m(V_{c0} - V_c) + V_{c0} W_{eff}(C_0 - C_m)} - C_m(V_c - V_{c0}) \right] \tag{20}$$

Since it is more convenient to express concentrations in units of C_{iso}, the concentration in units of relative tonicity, equation 20 is transformed with the substitutions, $C_{iso} = C_m/C_0$ and $\Delta V_c = (V_c - V_{c0})$:

$$t = \frac{V_{c0} W_{eff}}{P_w A C_{iso}^2 C_0} \left[\ln \frac{1 - C_{iso}}{1 - C_{iso}(1 + \Delta V_c / V_{c0} W_{eff}} - \frac{C_{iso} \Delta V_c}{V_{c0} W_{eff}} \right] \tag{21}$$

To determine P_w, ΔV_c is plotted against time in seconds for each experiment. P_w is obtained by superimposing the theoretical curves, calculated according to equation 21, into the experimental data and finding the best fit. A set of theoretical curves has to be made for each single fiber. Each set has been calculated for values of 1.0, 1.5, 2.0, 2.5, 3.0, and 4.0 for $P_w \times 10^{-2}$.

THE FILTRATION PERMEABILITY COEFFICIENT

Evaluation of equation 21 requires a knowledge of the fraction of cell water which is apparently free to participate in the osmotic phenomena (W_{eff}). W_{eff}, as defined by Ponder's (23) equation,[3] consists of two components: one the water content of the cell, and the other an empirical factor which might be in part due to "bound" water and/or rigidity of the cell membrane (24, 25). In collaboration with Dr. Flor V. Barnola we have obtained a value of

[3] Ponder's equation (reference 23, equation 3.11), derived for red cells, is $V = W_{eff}(1/T - 1) + 100$ in which V is the cell volume in a system in which the initial volume of the cell in an isotonic medium is denoted by 100. The tonicity, T, is defined as the ratio of the depression of the freezing point of the suspension medium to that of the isotonic medium. T is equivalent to C_{iso} in the present notation.

0.44 ± 0.06 for W_{eff} in 12 single fibers of *Doryteuthis plei* (Table VI), under similar experimental conditions.

The results of the P_w measurements are given in Table VII, a value of $1.9 \pm 0.3 \times 10^{-2}$ (cm.⁴/osM., sec.) has been obtained in a series of 8 experiments. Data from a typical experiment are shown in Text-fig. 7. It may be observed that the uncertainty in fitting the curve is $\pm 0.25 \times 10^{-2}$. As noticed, the standard deviation is in close agreement with the scale error factor. The

TABLE VI

MEASUREMENTS OF W_{eff} IN SINGLE AXONS OF THE SQUID

(Temperature 22–24°C.)

Exp. No.	V_c/V_{c0}	C_{iso}	W_{eff}
24	1.13	0.79	0.48
25	1.13	0.79	0.48
26	1.15	0.79	0.55
27	1.14	0.79	0.51
28	1.09	0.79	0.33
29	1.11	0.79	0.40
30	1.11	0.79	0.40
31	1.11	0.79	0.40
32	1.08	0.84	0.42
33	1.06	0.87	0.40
34	1.09	0.82	0.41
35	1.11	0.82	0.50
Average ± Std. Dev.			0.44 ± 0.06

TABLE VII

MEASUREMENTS OF FILTRATION PERMEABILITY COEFFICIENT IN SINGLE AXONS OF THE SQUID

(Temperature 22–24°C.)

Exp. No.	Axon radius	P_w	P_w (per cm. H_2O pressure)
	cm. × 10^{-2}	$\frac{cm.^4}{osM., sec.} \times 10^{-2}$	$\frac{ml.}{cm.^2, sec., cm.\ H_2O\ pressure} \times 10^{-10}$
24	1.88	2.5	10.0
25	1.85	2.0	8.0
26	1.55	2.0	8.0
27	1.56	2.0	8.0
28	1.65	2.0	8.0
29	1.51	1.5	6.0
30	1.97	1.5	6.0
31	1.97	2.0	8.0
Average ± Std. Dev.		1.9 ± 0.3	7.8 ± 1.3

filtration permeability coefficient, P_w, may also be expressed in Pappenheimer's units (26), P_w per cm. H_2O pressure, as $7.8 \pm 1.3 \times 10^{-10}$ ml./(cm.^{2}, sec., cm. H_2O pressure), as it is shown in Table VII. Hill (27), who has measured osmotic permeability in the giant axon of *Loligo pealii*, gives his results in terms of the time required to reach half the final volume. As he points out, these data depend upon the area and the volume of each nerve, and so cannot be compared directly with the present results. In order to show that our data are similar to his, it is necessary to compare two similar nerves in a bathing medium of the same tonicity, since equation 21 shows that C_{iso} must also be considered as a factor. In Hill's Table III (experiment 23, vi. 49) a half-time of 1.4 minutes was obtained for an axon of 290 μ diameter in an 80 per cent sea water solution. The data for Text-fig. 7 have been obtained

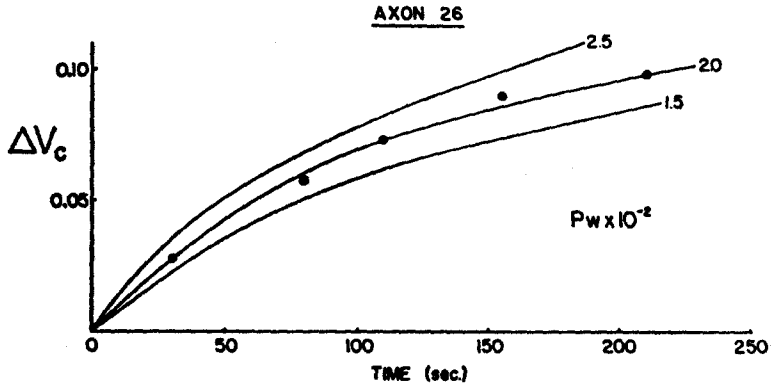

TEXT-FIGURE 7. Fit of experimental data with theoretical curves, calculated from equation 22 for $P_w \times 10^{-2}$ values of 1.5, 2.0, and 2.5; $C_{iso} = 0.80$. The points show experimental volume changes in an anisotonic medium represented as a function of time.

with an axon of 310 μ diameter (our Table VII, experiment 26). The half-time observed, 1.2 minutes, is in good agreement with Hill's result. Thus water entrance into the giant axon in these two species of squid is closely similar in osmosis, as in diffusion.

In some experiments, a zero time shift of up to 8 seconds has been observed; this has been attributed to delay in contact of the new environment with the membrane, due mainly to the connective tissue around the nerve. The zero time shift is similar to the half-time for water movement ($0.693/k_{23}$) from compartments 2 to 3 in the diffusion experiments. A similar phenomenon has been observed by Sidel and Solomon in red cells (22). These investigators have interpreted the time shift as due to the changes in pH or in NaCl concentration, which may also be operative in nerve. The pH change has been discarded in our observations.

Since both the Schwann cell and the axolemma lie between the extracellular space and the axoplasm, it is important to determine the part played by each barrier in maintaining the osmotic pressure gradient. In view of the 60 Å channels that cross the Schwann cell barrier it would seem reasonable to assume that the true barrier is provided by the axolemma. In order to establish this conclusion it is necessary to determine whether any osmotic pressure gradients may be maintained across channels of such large dimensions. Staverman (28) has analyzed the osmotic behavior of such leaky membranes; he describes the ratio of the osmotic pressure actually observed, π_{obs}, to the theoretical osmotic pressure, π_{th}, that would be developed across a truly semipermeable membrane in terms of a reflection coefficient, $\sigma = \pi_{obs}/\pi_{th}$.

Durbin, Frank, and Solomon (29) have suggested that $\sigma = 1 - (A_s/A_w)$, in which A_s and A_w are the restricted areas for filtration available for the solute and the water molecules respectively, and Durbin (30) has verified this relationship experimentally. Renkin (31) has presented a mathematical treatment by which A_s and A_w may be determined in terms of the ratio of a, the radius of the penetrating molecule, to r, the radius of the cylindrical pores, and has shown experimentally that his relationship describes filtration through small cylindrical pores. When the ratio $(a/r) \rightarrow 0$, the ratio (A_s/A_w) tends to approach 1 and σ approaches 0. Since the Schwann cell channels are not cylindrical pores, but rather long slits 5.3×10^4 Å long and 60 Å wide, friction with the walls is only important along one dimension; therefore, when Renkin's equation (reference 31, equation 19) is applied to these channels, it provides an upper limit for σ. The calculated σ for Na and Cl ions in pores of 60 Å width is only 0.09. Thus it seems clear that the Schwann cell channels are so large that no effective osmotic pressure can be developed across this cell layer. We may therefore conclude that the axolemma is the true barrier for water movement under an osmotic pressure gradient.

When an osmotic pressure gradient is applied, the Schwann cell itself might also swell. This problem has been approached directly by the electron microscope and has been presented in Section I (Figs. 8 and 9). When the nerve fiber is treated with the hypotonic medium and then fixed at the same hypotonicity ($C_{iso} = 0.80$), the channel lumen is occasionally interrupted. These structural changes obstruct the free path through the channel but do not appear to reduce it sufficiently to produce variation in the rate of swelling. Text-fig. 7 shows that the kinetics of swelling can be described by a single permeability coefficient over the whole time course. Thus the swelling of the Schwann cell appears to have no effect on osmotic water movement during our observation time, and the measured filtration permeability coefficient, P_w, may be assigned to the axolemma.

IV. *Limiting Value for Equivalent Pore Radius in the Axolemma*

Koefoed-Johnsen and Ussing (32) have considered differences between diffusion and osmotic permeabilities as indicative of the presence of water-filled pores in the cell membrane. The water diffusion coefficient of 1.42×10^{-4} cm./sec. when converted (17) to units of osmotic flow is 1.0×10^{-10} ml./(cm.^{2}, sec., cm. H_2O pressure). This is smaller by almost an order of magnitude than the osmotic permeability coefficient of 7.8×10^{-10} ml./(cm.^{2}, sec., cm. H_2O pressure).

An estimate of the equivalent pore radius in single cell membranes can be obtained by combining the two permeability constants according to the methods of Pappenheimer, Renkin, and Borrero (33), as has been done for the red cell membrane by Paganelli and Solomon (17). The equivalent pore radius is given (their equation 22) by:

$$r = -a + \sqrt{2a^2 + \lambda} \qquad (22)$$

in which $\lambda = \dot{M}_{H_2O} 8\eta D_{H_2O} / \dot{m}_{H_2O}$. The symbols have the following meanings:

$\dot{M}_{H_2O}$ = the volume rate of water bulk flow per unit pressure difference;
$\dot{m}_{H_2O}$ = the diffusion flow across the axolemma;
η = the viscosity of water, being equal to 9.36×10^{-3} poise at 23°C.;
D_{H_2O} = taken as the diffusion coefficient of $H^1{}_2O^{18}$ at 23°C., equal to 2.65×10^{-5} cm.^{2}/sec. (15);
a = the radius of the water molecule, taken as 1.5 Å (34).

The volume rate of water bulk flow per unit pressure, M_{H_2O}, is obtained by subtracting the diffusion flow component from the total osmotically induced water flow (29). In the present experiments the diffusion component of the osmotic flow across the axolemma is unknown but has been assumed to be larger than that determined for the Schwann cell channels. As a rough approximation $\dot{M}_{H_2O}$ can be taken as the total osmotic flow across the axolemma minus the diffusion flow through the Schwann cell channels, giving $\dot{M}_{H_2O} = 6.8 \times 10^{-10}$ ml. H_2O/(sec., cm.^{2}, cm. H_2O pressure). Equation 22 also requires a value for $\dot{m}_{H_2O}$ for the axolemma. Since the diffusion data refer to the Schwann cell channels, we do not have data from which $\dot{m}_{H_2O}$ may be determined exactly. However, $\dot{m}_{H_2O}$ must be greater than 1.42×10^{-4} cm./sec. so that $\lambda \leqq 95.1 \times 10^{-16}$ cm.^{2} and $r \leqq 8.5$ Å. A rough calculation will show that this figure is indeed a true maximum. If the axolemma had equivalent pores of 3.5 Å radius, similar to human red cells (17), $A_p/\Delta x$ for the axolemma would be three times larger than the value determined for the Schwann cell channels. This would increase $\dot{m}_{H_2O}$ by a factor of three, and reduce $\dot{M}_{H_2O}$ by about 20 per cent, which shows that λ decreases as $A_p/\Delta x$ increases.

The 8.5 Å maximum value is about half the equivalent pore radius calculated previously by Nevis (13) for the squid "nerve fiber." If large pores, as proposed by Nevis, were present in the axolemma, it would be difficult to correlate the pore radius with the low sodium and potassium conductances. As already pointed out, our experimental results are in excellent agreement with those of Nevis and Hill. An equivalent pore radius calculated by our method from their data would be identical with the value presented above. The higher value given by Nevis results from a different method of calculation, with which we do not agree.

The equivalent pore radius of the axolemma is bounded by two limits; it will be larger than 1.5 Å, the radius of the water molecule, and smaller than 8.5 Å. The presence of pores whose radius lies between these limits is compatible with restricted diffusion of Na and makes the axolemma typical of other single cell membranes as reviewed by Solomon (35).

SUMMARY

The electron microscope studies have revealed the presence of slit-like channels traversing the Schwann cells. These channels, 60 Å wide by 53000 Å long, wind tortuously through the Schwann cell along a path whose total length is 43000 Å, eight times greater than the average thickness of the Schwann cell. The axolemma itself is surrounded by a space, 83 Å thick, into which the channels discharge. (These values represent the average of the electron micrograph measurements plus a 15 per cent increase to correct for shrinkage produced by the methacrylate embedding.)

The resistance that these channels and this space offer to the diffusion of water may be described by the parameter, $A_w/\Delta x$. The value we have obtained, 5.3 cm., is in close agreement with the value of 4.0 cm. given by Frankenhaeuser and Hodgkin (9) to describe the extracellular resistance to the diffusion of K, thus leading to the supposition that the pathway for water and K is the same until they reach the axolemma surface.

The Schwann cell and the axolemma discharge complementary functions. The Schwann cell is traversed by channels which allow water and ions to reach the axolemma. These channels provide the major route of access to the axolemma surface. The axolemma is the barrier for osmotically induced water flow into the axoplasm. This finding is consonant with the presence of small pores in the axolemma, of diameter comparable with the hydrated ionic radius of Na. Thus, the present results are wholly compatible with the controlled ionic environment which is responsible for the normal functioning of the nerve.

Our thanks are due to Professors A. K. Solomon and A. L. Hodgkin for reading the manuscript and for their helpful suggestions. Some of the experiments presented in Section III have been successful

owing to the assistance of Dr. Flor V. Barnola, to whom we wish to express our particular indebtedness. We are also grateful to Dr. Guillermo Whittenbury and Lic. Alberto Serra, for valuable discussions in the course of the work.

BIBLIOGRAPHY

1. HODGKIN, A. L., *Proc. Roy. Soc. London, Series B*, 1958, **148**, 1.
2. PALADE, G. E., *J. Exp. Med.*, 1952, **95**, 285.
3. LUFT, J. H., *J. Biophysic. and Biochem. Cytol.*, 1957, **2**, 799.
4. HODGKIN, A. L., and KATZ, B., *J. Physiol.*, 1949, **108**, 37.
5. BORISKO, E., *J. Biophysic. and Biochem. Cytol.*, 1956, **2** (suppl.), 3.
6. FERNÁNDEZ-MORÁN, H., *J. Biophysic. and Biochem. Cytol.*, 1956, **2** (suppl.), 29.
7. SJÖSTRAND, F. S., *Exp. Cell Research*, 1958, **10**, 657.
8. GEREN, B. B., and SCHMITT, F. O., *Proc. Nat. Acad. Sc.*, 1954, **40**, 863.
9. FRANKENHAEUSER, B., and HODGKIN, A. L., *J. Physiol.*, 1956, **131**, 341.
10. VILLEGAS, G. M., and VILLEGAS, R., *J. Ultrastructure Research*, in press.
11. VILLEGAS, R., and VILLEGAS, G. M., II Symposium Interamericano sobre la Aplicación de la Energía Nuclear para Fines Pacíficos, Buenos Aires, 1959, Organización de los Estados Americanos, Washington, in press.
12. VILLEGAS, R., *Proceedings of the XXI International Congress of Physiological Sciences*, Buenos Aires, 1959, 289.
13. NEVIS, A. H., *J. Gen. Physiol.*, 1958, **41**, 927.
14. JACOBS, M. H., *Ergebn. Biol.*, 1935, **12**, 1.
15. WANG, J. H., ROBINSON, C. V., and EDELMAN, I. S., *J. Am. Chem. Soc.*, 1953, **75**, 466.
16. ROUGHTON, F. J. W., *Proc. Roy. Soc. London, Series B*, 1932, **111**, 1.
17. PAGANELLI, C. V., and SOLOMON, A. K., *J. Gen. Physiol.*, 1957, **41**, 259.
18. VILLEGAS, R., BARTON, T. C., and SOLOMON, A. K., *J. Gen. Physiol.*, 1958, **42**, 355.
19. HUXLEY, A. F., *in* Mineral Metabolism (C. L. Comar and F. Bronner, editors), New York, Academic Press, Inc., in press.
20. KOECHLIN, B. A., *J. Biophysic. and Biochem. Cytol.*, 1955, **1**, 511.
21. JACOBS, M. H., *in* Modern Trends in Physiology and Biochemistry (E. S. Guzmán Barron, ed.), New York, Academic Press, Inc., 1952, 149.
22. SIDEL, V. W., and SOLOMON, A. K., *J. Gen. Physiol.*, 1957, **41**, 243.
23. PONDER, E., Hemolysis and Related Phenomena, New York, Grune and Stratton, 1948, 85.
24. DRABKIN, D. L., *J. Biol. Chem.*, 1950, **185**, 231.
25. TEORELL, T., *J. Gen. Physiol.*, 1952, **35**, 669.
26. PAPPENHEIMER, J. R., *Physiol. Rev.*, 1953, **33**, 387.
27. HILL, D. K., *J. Physiol.*, 1950, **111**, 304.
28. STAVERMAN, A. J., *Rec. trav. chim. Pays-bas*, 1951, **70**, 344; 1952, **71**, 623.
29. DURBIN, R. P., FRANK, H., and SOLOMON, A. K., *J. Gen. Physiol.*, 1956, **39**, 535.
30. DURBIN, R. P., *Proceedings of the First National Biophysics Conference*, New Haven, Yale University Press, 1959, 323.

31. RENKIN, E. M., *J. Gen. Physiol.*, 1954, **38**, 225.
32. KOEFOED-JOHNSEN, V., and USSING, H. H., *Acta Physiol. Scand.*, 1953, **28**, 60.
33. PAPPENHEIMER, J. R., RENKIN, E. M., and BORRERO, L. M., *Am. J. Physiol.*, 1951, **167**, 13.
34. MORGAN, J., and WARREN, B. E., *J. Chem. Physics*, 1938, **6**, 666.
35. SOLOMON, A. K., *Proceedings of the First National Biophysics Conference*, New Haven, Yale University Press, 1959, 314.

PLATE 1

FIGURE 1. Low resolution electron micrograph of the squid giant fiber showing the dense axoplasm (axon = *A*) with numerous profiles belonging to the endoplasmic reticulum (*er*), and the Schwann cell (*SC*) bounded on its outer surface by the basement membrane (*bm*). Several mitochondria (*m*) and the osmiophilic double lines (*ol*) appear inside the Schwann cell cytoplasm. The connective tissue (*CT*) is seen covering the basement membrane on its outer side.
FIGURES 2 and 3. Electron micrograph of the axon covers. The Schwann cell cytoplasm shows the characteristic paired osmiophilic lines (*ol*) running parallel to the surface. The basement membrane (*bm*) is seen as a homogeneous strip sheathing the outer surface of the Schwann cell. Note the connective tissue (*CT*) at the top.

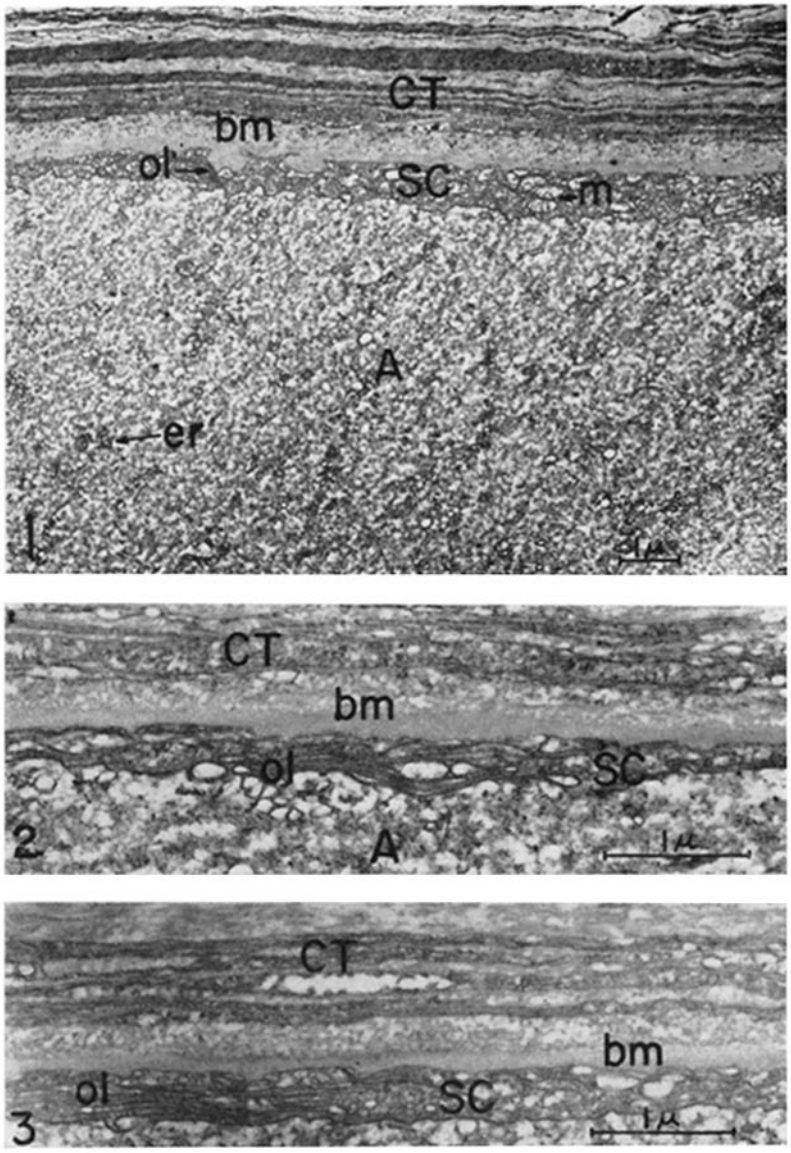

VILLEGAS AND VILLEGAS *Membranes in Nerve Fiber of Squid*

PLATE 2

FIGURES 4 and 5. Cross-sections of the giant fiber showing axon (*A*), Schwann cell (*SC*), basement membrane (*bm*), and connective tissue (*CT*). Mitochondria (*m*) and numerous profiles belonging to the endoplasmic reticulum (*er*) can be seen in the axoplasm. The arrows show both ends (*o*) of one channel (*ch*) running across the Schwann cell cytoplasm. Other channels can be seen opening only at the outer surface of the Schwann cell. The endoplasmic reticulum (*er*) and microsomes are also shown in the Schwann cell cytoplasm.

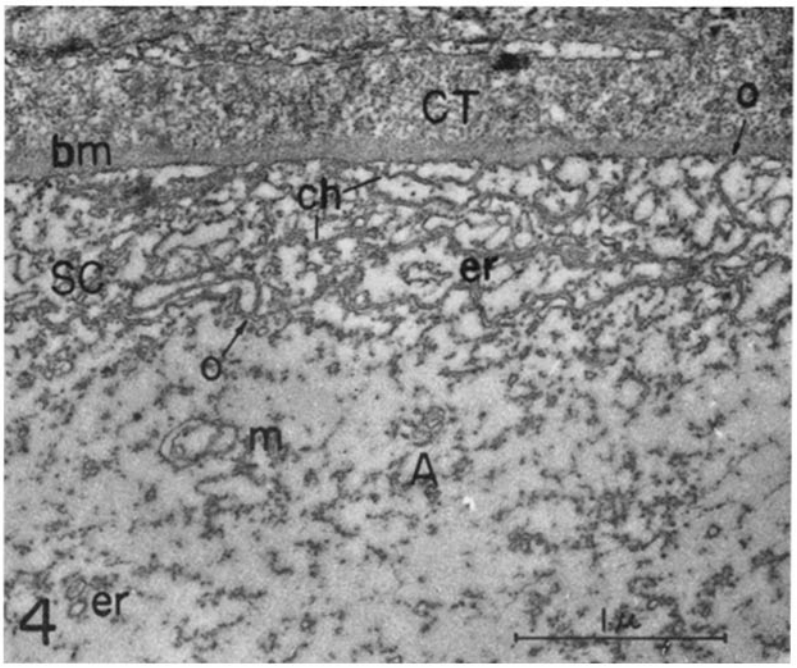

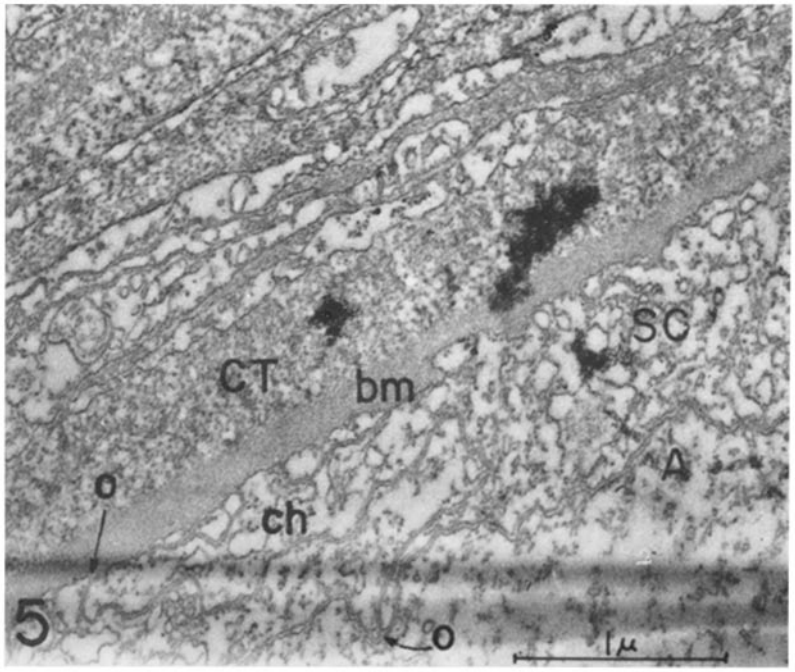

VILLEGAS AND VILLEGAS *Membranes in Nerve Fiber of Squid*

PLATE 3

FIGURES 6 and 7. High resolution electron micrographs of the permanganate-fixed material, showing a cross-section through the Schwann cell (*SC*). The channels (*ch*) are formed by invaginations of the Schwann cell membrane on both the axonal and outer surfaces (arrows); axolemma = *a*; a branching or fusion of the channels is seen at (*b*) in Fig. 6. Each channel is formed by two unit membranes separated by the lumen. Each unit membrane appears as a dense double line with a less dense interstice (see low right insert).

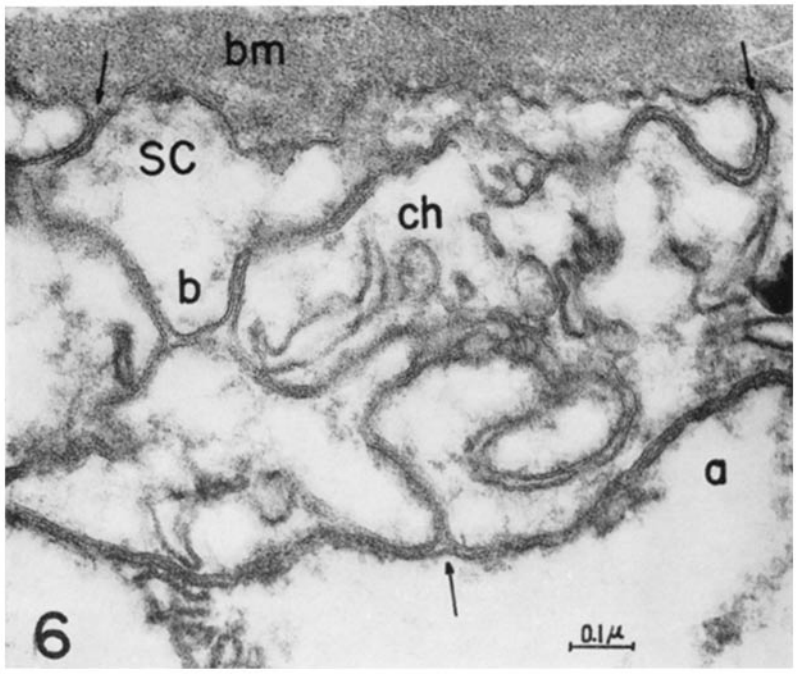

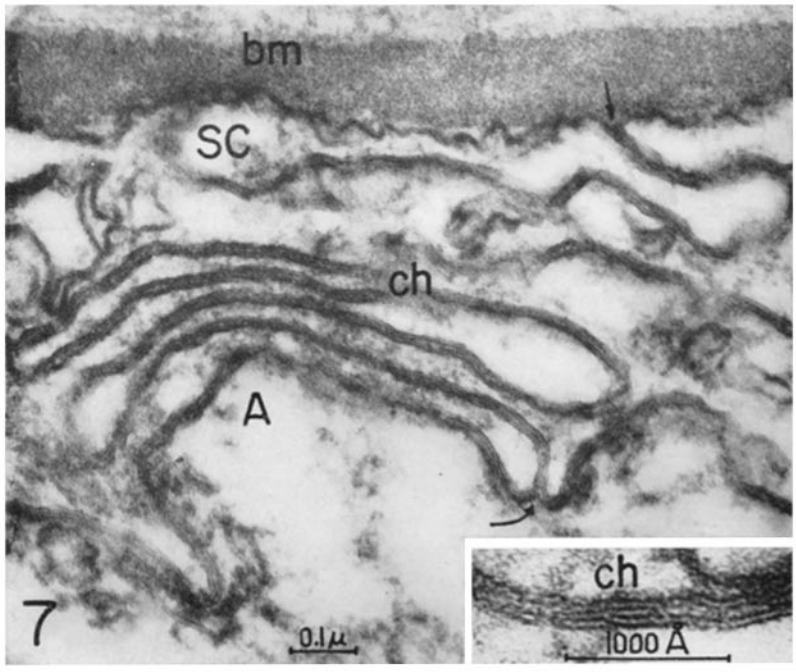

VILLEGAS AND VILLEGAS *Membranes in Nerve Fiber of Squid*

PLATE 4

FIGURES 8 and 9. Electron micrographs of the hypotonic permanganate-fixed material showing the channels (*ch*) across the Schwann cell cytoplasm (*SC*). The arrows show the points at which the channel lumen appears to be closed (*c ch*), the axolemma (*a*) and the axon (A). (For explanation see text.)

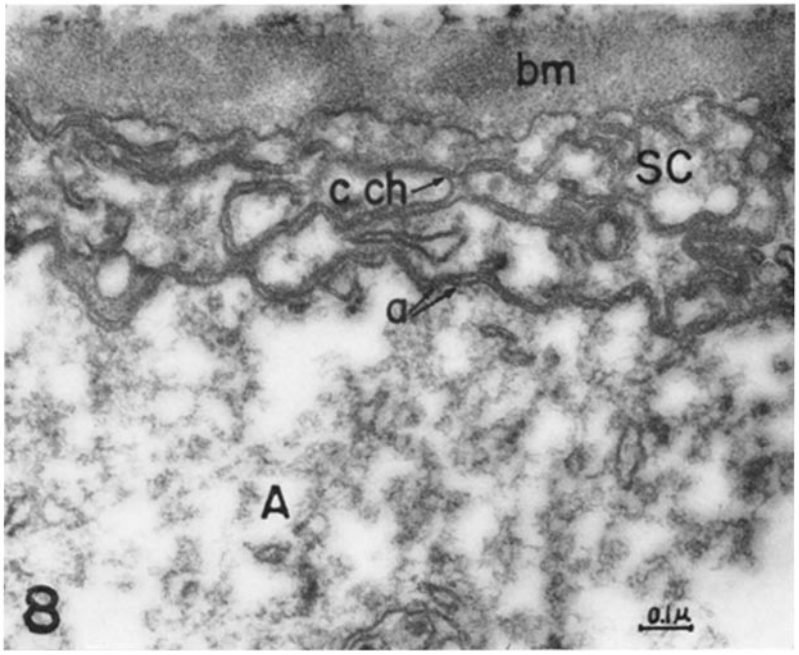

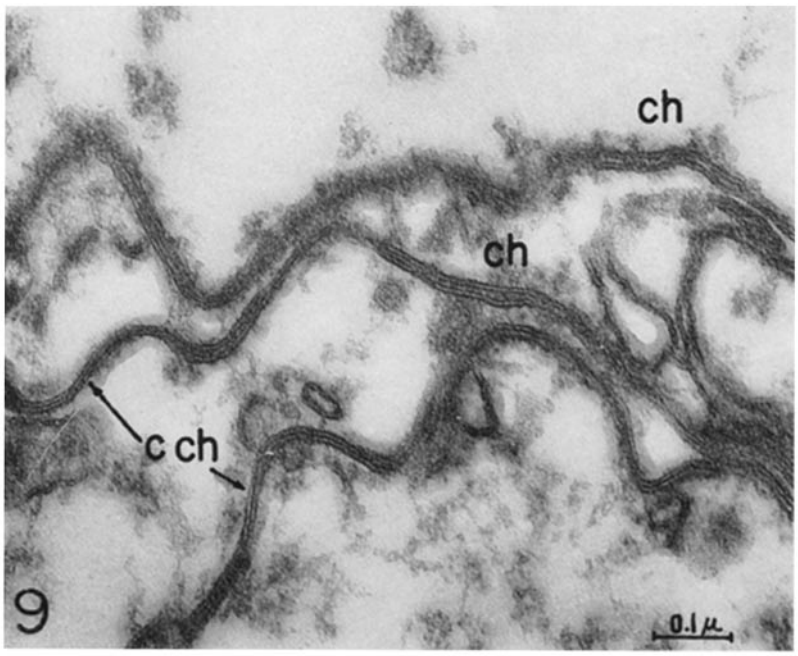

VILLEGAS AND VILLEGAS *Membranes in Nerve Fiber of Squid*